COMMUNICATION

ChemComm
www.rsc.org/chemcomm

Solid–solid transformation mechanism for nanocrystalline sodalite from pillared clay

Jin–Ho Choy,*[a] Sung-Reol Lee,[a] Yang-Su Han,[a] Man Park[a] and Gyeong-Su Park[b]

[a] *National Nanohybrid Materials Laboratory, School of Chemistry and Molecular Engineering, Seoul National University, Seoul 151–747, Korea. E-mail: jhchoy@plaza.snu.ac.kr; Fax: (+82)2–872–9864; Tel: (+82)2–880–6658*

[b] *Samsung Advanced Institute of Technology, Post Office Box 111, Suwon 440-660, Korea*

Received (in Cambridge, UK) 28th April 2003, Accepted 11th June 2003
First published as an Advance Article on the web 30th June 2003

We here report the synthesis of nanocrystalline sodalite by a solid–solid transformation from a solid gel mixture of Al_2O_3 pillared montmorillonite (Al_2O_3-PILM) and NaOH under an ambient atmosphere at 80 °C. HR-TEM clearly shows both the formation of sodalite nuclei by the solid–solid transformation of the montmorillonite matrix and the crystal growth of nanocrystalline sodalite through the rearrangement of delocalized nuclei.

Zeolites including sodalites are synthesized from hydrogels of amorphous aluminosilicate precursors under hydrothermal conditions, although they also result from the crystalline precursors.[1–6] In this system, nucleation and subsequent crystal growth take place through solution-mediated transport after an induction period.[2–5,7–10] On the other hand, it is also possible for zeolites to be crystallized from an amorphous solid phase through solid–solid transformation. However, the solid–solid transformation mechanism is not well understood to date, although incessant efforts have been directed at the exploitation of zeolite synthesis by solid–solid transformations and the elucidation of their mechanisms in heterogeneous systems.[6,9–13] Here we report unequivocal evidence for delocalized nucleation in a solid–solid transformation and confined crystal growth through nucleus–nucleus rearrangement from a solid gel mixture of Al_2O_3-PILM and NaOH. Furthermore, this non-hydrothermal system results in a nanocrystalline sodalite with a discrete particle size distribution.

Al_2O_3-PILM was prepared by a conventional ion exchange reaction between the interlayer Na^+ ions in montmorillonite (Kunipia F, $((Na_{0.35}K_{0.01}Ca_{0.02})(Si_{3.89}Al_{0.11})(Al_{1.60}Mg_{0.32}Fe_{0.08})O_{10}(OH)_2nH_2O$, cation exchange capacity = 100 meq per 100 g) and Al-polyhydroxy cation ($[Al_{13}O_4(OH)_{24}(H_2O)_{12}]^{7+}$, Keggin-type ions). The intercalated Al-polyhydroxy cations were converted to Al_2O_3 by heating at 400 °C for 4 h in air. For the synthesis of nanocrystalline sodalite, a pillared clay gel prepared by the addition of 25 wt% water was well mixed with solid NaOH with a typical mole ratio of $[OH^-]/[Si] = 10$. The resulting solid gel mixture was thermally treated at 80 °C under ambient atmospheric conditions. In order to investigate the transformation process from Al_2O_3-PILM to sodalite at 80 °C, a part of the reaction product was removed periodically from the reaction mixture, and used for subsequent analyses.

Fig. 1 shows the evolution of XRD patterns of the sodalite phase from the solid gel mixture of Al_2O_3-PILM and NaOH (s) at 80 °C as a function of reaction time. The Al_2O_3-PILM exhibits a series of (00*l*) diffraction patterns which confirm the formation of a regular intercalation compound with a basal spacing of 18.5 Å. After reaction for 30 min, the (00*l*) diffraction lines of Al_2O_3-PILM shift to the higher 2θ angles (d = 12.8 and 6.4 Å), indicating the collapse of interlayer pillars. At the same time, new diffraction peaks corresponding to the sodalite phase appear. It is worthy of note here that the crystalline sodalite phase is formed even within 30 min without the formation of X-ray amorphous phases, which is fundamentally different from the previous results reported in the literature.[5–10] Such a rapid formation of sodalite is surely due to the homogeneous distribution of Si and Al as well as the well-developed micropores of Al_2O_3-PILM (S_{BET} = ~ 245 $m^2\ g^{-1}$). The former enables the aluminosilicate network to be converted into a sodalite framework through a solid–solid transformation, while the latter allows the rapid diffusion of hydrated NaOH to facilitate zeolite formation without any noticeable perturbation of the pristine layer structure of montmorillonite. As the reaction proceeds, the crystalline sodalite phase becomes dominant at the expense of Al_2O_3-PILM, and single phase sodalite is eventually formed after a reaction at 80 °C for 180 min. In contrast to the conventional solution-mediated transport processes for crystal growth,[9–10,14–15] the absence of a distinct X-ray amorphous stage implies that the transformation does not take place through long-range diffusion of dissolved aluminium and silicon species but through a short-range molecular-level rearrangement.

The rapid incorporation of Al into the silicate network through the solid–solid transformation is reflected in the FT-IR spectra (Fig. 2). A remarkable and gradual red shift of the Si–O stretching vibration 1100 cm^{-1} to 986 cm^{-1} is observed along with a weakening of the absorption bands at 3630 cm^{-1} and 920 cm^{-1}, which are associated with the structural hydroxy groups in the octahedral sheets of the clay layer. Other diagnostic features of the sodalite formation are the appearance of a new absorption peak at 430 cm^{-1} due to the formation of a single four-membered ring (S4R) of sodalite units, and a gradual reduction of the intensity of the peak at 524 cm^{-1} assigned to the Si–O–Al bending vibration in clay.[7,16]

Sodalite formation through solid–solid transformation is clearly confirmed by high resolution transmission electron microscopy (HR-TEM). Fig. 3(a) shows the typical HR-TEM images of a thin-sectioned Al_2O_3-PILM oriented with its *ab* planes parallel to the optical axis of the microscope. The clay layers are discernible as the solid dark lines while the pores appear as a lighter contrast between layers. After reaction at 80

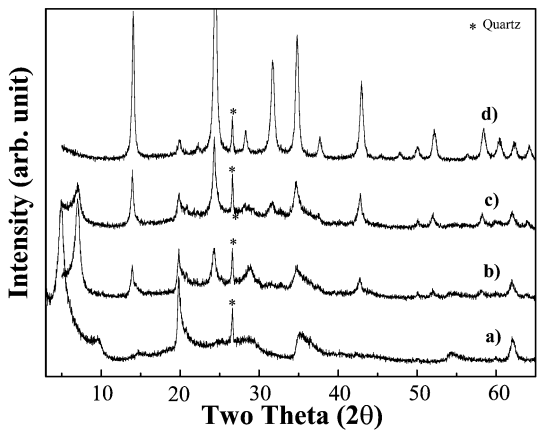

Fig. 1 Powder X-ray diffraction patterns of a) Al_2O_3-PILM and the reaction products obtained by solid–solid transformation at 80 °C under an ambient atmosphere for b) 30 min, c) 50 min, and d) 180 min. A small amount of quartz initially present in the starting montmorillonite is always visible (2θ = 26.5°) throughout the reaction.

DOI: 10.1039/b304638a

°C for 30 min (Fig. 3(b)), a new lattice fringe appears randomly in the crystalline region. The arrow highlights the highly ordered lattice fringe of the sodalite nuclei, indicating that the image of the partially transformed region is eventually transformed into a well-developed lattice with respect to the reaction time. Further inspection illustrates the course of the nucleation and crystal growth mechanism in the heterogeneous system (circled). Sodalite nuclei are randomly delocalized over the entire region. The rearrangement of the delocalized sodalite nuclei occurs successively and leads to the long-range lattice fringes of sodalite. As the reaction proceeds, the long-range lattice fringes become dominant instead of the dislocated lattice phases. Fig. 3(c) shows a fully crystalline lattice fringe of sodalite obtained after 180 min. HR-TEM images clearly demonstrate that the formation of sodalite nuclei takes place simultaneously from an aluminosilicate matrix by the localized solid–solid transformation of the clay lattice, and that the rapid crystal growth takes place through the rearrangement of sodalite

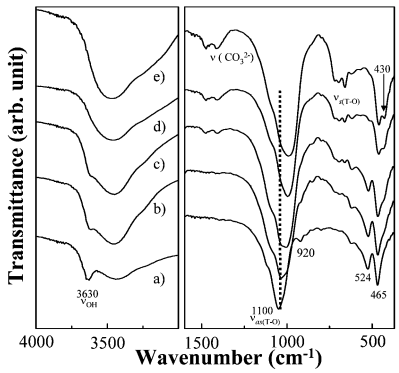

Fig. 2 IR spectra of a) Al_2O_3-PILM and the solid products obtained by solid–solid transformation at 80 °C under an ambient atmosphere for b) 30 min, c) 50 min, d) 100 min, e) 180 min.

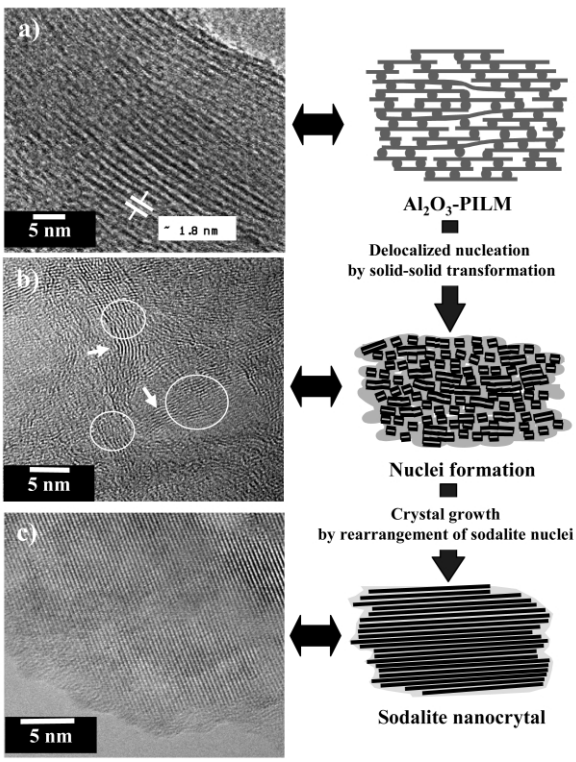

Fig. 3 TEM images of a) Al_2O_3-PILM and the solid products obtained at 80 °C for b) 30 min and c) 180 min, and a schematic representation of the proposed sodalite growth mechanism by solid–solid transformation.

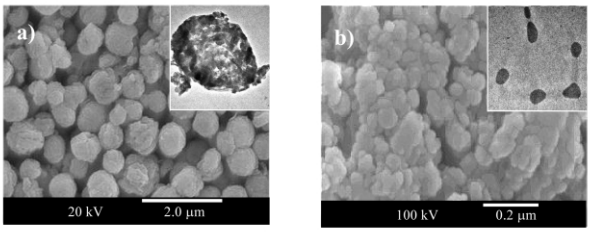

Fig. 4 SEM images of a) the spherical particles obtained from Al_2O_3-PILM and b) sodalite nanocrystals dispersed by using ultrasonication. The insets show the TEM images of the respective samples.

nuclei with a limited dimension to result in nanocrystalline sodalite with a discrete particle size distribution.

A schematic illustration of the solid–solid transformation process in this system is as follows (Fig. 3). The fast diffusion of hydrated NaOH into two-dimensional clay layers results in the formation of aluminosilicate species upon the collapse of the Al_2O_3 pillars and the delocalized sodalite nucleation by the solid–solid transformation. As the reaction proceeds, intermediate particles of nanometre size are formed by the finely cracked division of layered aluminosilicate particles. At the same time, the crystallization of sodalite takes place mainly by the rearrangement of sodalite nuclei present in the finely cracked particles. Fig. 4 shows scanning electron micrographs with transmission electron micrographs (inset) of sodalite particles obtained from Al_2O_3-PILM. The spherical particles composed of nanometre-sized sodalite crystals are very uniform with lamellar character. The sodalite nanocrystals are readily obtained by ultrasonication, and their homogeneous suspension is quite stable (Fig. 4(b)).

In this study, it is clearly shown that sodalite crystallization takes place by a solid–solid transformation. A solution-mediated reaction could not be involved in both nucleation and crystal growth of the nanocrystalline sodalite. In addition, our solid–solid transformation route could be applied to the preparation of nanocrystalline sodalite crystals with a discrete particle size distribution.

This work was supported by the Korean Ministry & Science Technology through National Research Laboratory (NRL) project' 99. Authors thank to the Ministry of Education for the Brain Korea 21 fellowship.

Notes and references

1 R. M. Barrer, *Hydrothermal Chemistry of Zeolites*, Academic Press, London, 1982.
2 J. M. Newsam, *Science*, 1986, **31**, 1093.
3 M. E. Davis, *Ind. Eng. Chem. Res.*, 1991, **30**, 1675.
4 G. A. Ozin, A. Kuperman and A. Stein, *Angew. Chem., Int. Ed .Engl.*, 1989, **28**, 359.
5 R. Aiello and E. Franco, *Rend. Accad. Sci. Fis. Mat., Naples*, 1968, **35**, 1.
6 J. Rocha and J. Klinowski, *J. Chem. Soc., Faraday Trans.*, 1991, **87**, 3091.
7 D. M. Bibby and M. P. Dale, *Nature*, 1985, **317**, 157.
8 B. Herreros and J. Klinowski, *J. Chem. Soc., Faraday Trans.*, 1995, **91**, 1147.
9 S. Mintova, N. H. Olson, V. Valtchev and T. Bein, *Science*, 1999, **283**, 950.
10 S. Mintova, N. H. Olson, J. Senker and T. Bein, *Angew. Chem., Int. Ed.*, 2002, **41**, 2558.
11 D. P. Serrano and R. Van Grieken, *J. Mater. Chem.*, 2001, **11**, 2391.
12 C. L. Choi, M. Park, D. H. Lee, J.-E. Kim, B.-Y. Park and J. Choi, *Environ. Sci. Technol.*, 2001, **35**, 2812.
13 D. P. Serrano, R. Van Crieken, P. Sanchez, R. Sanz and L. Rodriguez, *Microporous Mesoporous Mater.*, 2001, **46**, 35.
14 Gualtieri, P. Norby, G. Artioli and J. Hanson, *Microporous Mater.*, 1997, **9**, 189.
15 D. Akolekar, A. Chaffee and R. F. Howe, *Zeolites*, 1997, **19**, 359.
16 M. J. Wilson, *Clay Mineralogy: Spectroscopic and Chemical Determinative Methods*, Chapman & Hall, London, 1994.